INTERNATIONAL JOURNAL OF AUTOMOTIVE AND MECHANICAL ENGINEERING (IJAME)
ISSN: 2229-8649 e-ISSN: 2180-1606
VOL. 19, ISSUE 1, 9593 – 9605
DOI: https://doi.org/10.15282/ijame.19.1.2022.21.0740

ORIGINAL ARTICLE

Development of Automatic Ladder Climbing Inspection Robot Using Extension Type Flexible Pneumatic Actuators

S. Shimooka[1,*], K. Katayama[2], T. Akagi[2], S. Dohta[2], T. Shinohara[2], T. Kobayashi[2] and M. Aliff[3]

[1]Okayama University, 3-1-1 Tsushima-naka, Kita-ku, Okayama 700-0082, Japan
Phone: +81-086-251-8228
[2]Okayama University of Science, 1-1, Ridai-cho, Kita-ku, Okayama, 700-0005, Japan
Phone: +81-86-256-9786; Fax: +81-86-255-3611
[3]Malaysian Institute of Industrial Technology, Universiti Kuala Lumpur, Persiaran Sinaran Ilmu, Bandar Seri Alam, 81750 Johor, Malaysia

ABSTRACT – Recently, old and dilapidated infrastructures such as bridges, chimneys and tunnels have become very serious in Japan. Inspection of the infrastructure was done by climbing the ladders that were set up. However, the inspection becomes dangerous as it is necessary to climb into very high areas and unpredictable weather and conditions. In this study, a lightweight inspection robot that can climb ladders in adverse weather conditions was proposed and tested. To grasp a ladder pillar without hurting, the wrapping motion is required. Therefore, the flexible robot arm that can grasp the ladder pillar while approaching and release it while going away was also proposed and tested. The automatic ladder-climbing inspection robot that consists of two pillar grasping flexible robot arms and a lifting robot arm was proposed and tested. The control system of the robot, driven by four on/off valves and an embedded controller, was also constructed. The ladder climbing experiment using the tested robot was carried out. As a result, it could be confirmed that the robot can climb up and down a ladder with soft gripping the ladder, and the soft robot can be also operated by using only four valves.

ARTICLE HISTORY
Received: 20th April 2021
Revised: 1st April 2022
Accepted: 14th April 2022

KEYWORDS
Automatic ladder climbing robot;
Grasping flexible robot arm;
Extension type flexible;
Pneumatic actuator;
Embedded controller

INTRODUCTION

Recently, old and dilapidated infrastructure such as bridges, chimneys and tunnels have become very serious in Japan. In particular, the dilapidated condition of the bridge is around 717000 places in 2019, and this number is increasing every year and will endanger local users. According to a public investigation, it is expected that bridges that exceed a 50 -years lifespan will be more than 50 % by 2033 [1]. Therefore, the government, together with researchers need to immediately find solutions to avoid accidents [2]. Based on this problem, the inspection for checking cracks and strengths of chimneys becomes mandatory once every five years by the Ministry of Land, Infrastructure and Transport in Japan [3]. As a general survey of the chimney, a visual inspection for cracks, a strength inspection for concrete, and a thermographic inspection using an infra-red ray for deterioration are carried out. In this study, we aim to carry out a visual inspection for cracks using the robot. Nowadays, the inspection tendency is to use the unmanned aerial vehicle (UAV). However, UAV is much-affected weather conditions such as strong wind and rain. In addition, many inspections require hammering test. Therefore, professional investigators still climb the ladder installed in the building for inspection. In particular, the inspection of aged chimney, as shown in Figure 1 [4] is more dangerous. As higher position of chimney without other building is more affected by winds, UAV is more difficult to be used. In this case, the ladder-climbing robot is useful. As a ladder-climbing robot, Honda R&D Co., Ltd. developed the humanoid robot “E2-DD” for inspection and disaster support [8,9]. The robot has a height of 1.68 m and a weight of 85 kgf. The robot can work for about 90 minutes and climb the ladder at a speed of 4 km/h. Hashimoto also developed a robot that can climb ladder faster while supporting two points [10]. The humanoid robot has a height of 1.29 m and a weight of 110 kgf. Both of these robots are used for inspection and support during disasters. However, they are too heavy for climbing a deteriorated ladder. It causes a serious accident when the robot falls from the ladder. In addition, the robot rigid manipulator might hurt deteriorated ladders. Both robots also need long time to climb a ladder. On the other hand, Y. Funabora developed a UAV with an automatic inspection system [11,12]. However, these robots can not inspect under the condition of strong wind and rain. It is necessary to develop a lightweight and compact robot that can climb the ladder while holding ladder surely without causing damage to the ladder.

In this study, we aim to develop a lightweight automatic ladder-climbing inspection robot that can be used in windy and rainy conditions and driven by simple valve operation. The target robot must not give damage to the deteriorated ladder. In addition, to climb a ladder by easy operation, a flexible robot arm that can grasp the ladder pillars while approaching and release it while away must be operated by a few control signals. In detail, it means that the robot arm should be controlled by using one or two on/off signals. In order to use the robot in windy conditions, the robot needs to hold both pillars and a step surely. A pneumatic soft actuator is useful, because the pneumatic actuator has properties of

*CORRESPONDING AUTHOR | S. Shimooka | ✉ shimooka@okayama-u.ac.jp

lightweight, high ratio of generated force to mass and compliance based on air compressibility, compared with the electric motor. The typical electric robot arm needs a lot of joints driven by servo motors [8-10,13]. Therefore, we aim to develop a flexible robot arm using a few soft pneumatic actuators. As a soft pneumatic actuator, in the previous study, we developed an Extension type Flexible Pneumatic Actuator (we call it "EFPA" for short) that can extend about 2.5 times from its initial length [14-16]. The pipe inspection robot and rehabilitation device using EFPAs that could be used in water were developed [17,18]. The reinforced extension type EFPA with circumferential restraints was also developed for rehabilitation device of upper limbs [19]. The improved EFPA can realize the bending toward various radial directions and the extension. In this paper, two types of grasping actuators that can grasp and release various objects will be proposed and tested. The characteristics of the proposed actuators are investigated. Based on the experimental results, a flexible robot arm that can grasp the ladder pillars while approaching and release it while away by using two on/off valves is proposed. In detail, the robot arm needs both motions for wrapping and bending backwards. In addition, an automatic ladder-climbing inspection robot that consists of two pillar grasping flexible robot arms and a lifting robot arm using reinforced extension type EFPA with circumferential restraints is proposed. A control system of the robot-driven by four on/off valves and an embedded controller is also proposed. A ladder-climbing experiment using the tested robot is carried out.

Figure 1. View of cracked chimney [4].

PREVIOUS REINFORCED EFPA

Figure 2 shows the view and schematic diagram of EFPA developed in the previous study [14-16]. The EFPA consists of a silicone rubber tube covered with a bellows type nylon sleeve. The sleeve is not special equipment and is sold as an ordinal water supply hose (The Fit Life Co. Ltd., Hose Reel). The actuator can be easy to construct and make at a low cost. The rubber tube in the sleeve has an inner diameter of 8 mm, an outer diameter of 11 mm, the original length of 200 mm, and a mass of 50 g. The material cost of the actuator is very low, that is about 5 US dollars per 1 m. The actuator can extend until about 253% of its original length when the input pressure of 500 kPa is applied. The maximum pulling force of the actuator is about 60 N [16]. The pulling force of the actuator depends on the elastic property of the rubber tube, and it is related to the material and thickness of the rubber tube. The displacement of the actuator is inversely proportional to the thickness of the rubber tube. The pushing force of the developed actuator could not measure sufficient because of lower bending stiffness.

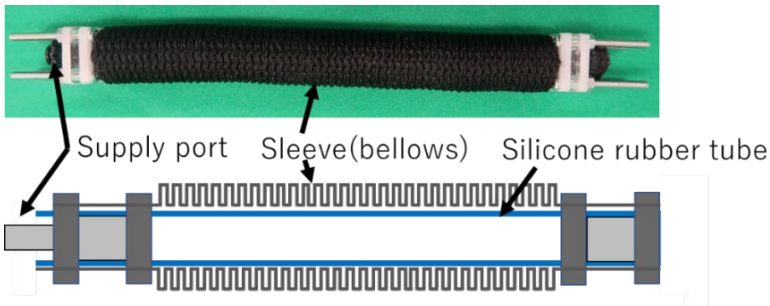

Figure 2. View and schematic diagram of EFPA [15-17].

To increase the stiffness of EFPA, the improved EFPA was developed in the previous study. Figure 3 and 4 show the view and schematic diagram of the reinforced EFPA with circumferential restraints; we call it "reinforced EFPA" for short [19]. The reinforced EFPA that consists of parallel arranged three EFPAs, as shown in Figure 4 is restrained each other by small circumferential restraint plates as shown in Figure 5. Each restraint plate with a thickness of 1 mm is inserted into the bellows of sleeve in EFPA, and it makes each actuator keep so as to arrange every 120 deg., at a radius of 12.5 mm from the center of the actuator. The reinforced EFPA could extend by applying a supply pressure to three EFPAs, and it could bend by applying a supply pressure to one or two EFPAs. The reinforced EFPA can also grasp an

object by giving a bending motion. In the next step, we aim to develop a grasping actuator that can realize both grasping and releasing an object by using two on/off valves.

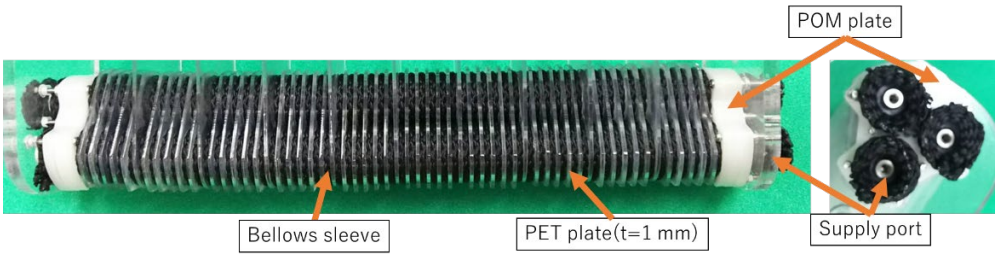

Figure 3. View of reinforced EFPA [19].

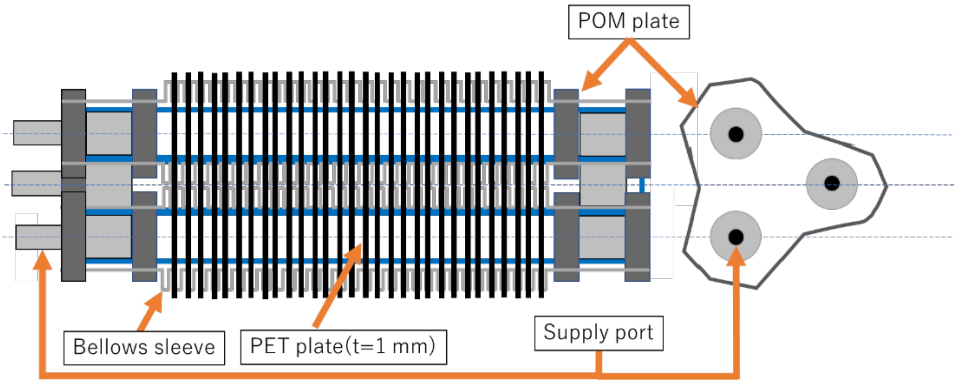

Figure 4. Schematic diagram of reinforced EFPA [19].

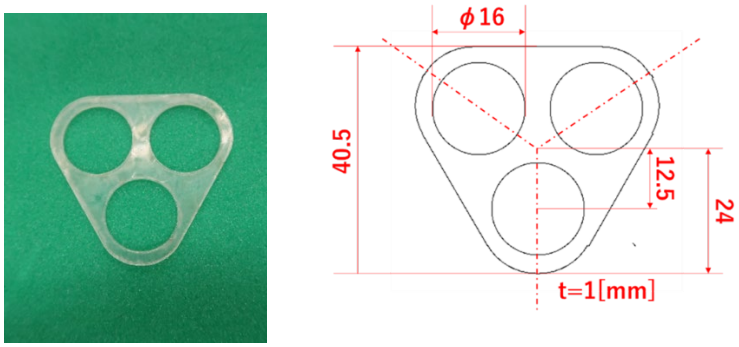

Figure 5. Shape of reinforced PET plate.

GRASPING ACTUATOR USING EFPA

Required Function of Grasping actuator using EFPAs

To realize both grasping and releasing the object using only one actuator, the actuator needs to deform helical shape and grasp the object by wrapping such as an elephant nose and an octopus leg. The actuator also needs to deform straight shape for releasing. In addition, the actuator needs to grasp the object softly so as not to give damage to the object. It is also necessary to develop the required actuator mentioned above that can be driven by using only two on/off valves. By using two on/off valves connected with two EFPAs independently, as a valve can work for supply and exhaust, four types of motions can be realized. As a result, we considered the following required functions as the desired actuator.

i. The actuator can deform both helical and straight shapes to realize both grasping and releasing.
ii. The actuator can realize the desired motion by using two on/off valves.
iii. The actuator is flexible so as not to give damage to the object.
iv. The actuator without any input energy can hold the object, that is, the actuator is helical in default.

Inner Circumferential Reinforced Helical EFPA(ICH-EFPA)

According to these requirements, a helical shaped actuator based on the reinforced EFPA with circumferential restraints was proposed and produced. Basic configuration of the actuator is as same as the reinforced actuator. Compared with the typical reinforced actuator, to realize the helical shaped actuator, the outer circumferential side EFPA is reinforced every four bellows, and inner circumferential side EFPA is reinforced every one bellows. In this study, two types of helical shaped actuators were proposed and tested. One is an inner circumferential reinforced helical EFPA; we call it “ICH-EFPA” for short, while an outer circumferential reinforced helical EFPA we call it “OCH-EFPA” for short.

Figure 6(a) and 6(b) show the view of the ICH-EFPA and the shape of the restraint plate, respectively. In the ICH-EFPA, two EFPAs are arranged on the inner circumferential side and one EFPA is arranged on the outer circumferential side. In addition, compared with the previous restraint plate of typical reinforced EFPA, the novel restraint plate has a smaller hole with a diameter of 14.5 mm for setting EFPA and they are set on circle with a smaller radius of 11 mm from the center. The length of EFPA A and B on the inner circumferential side is 560 mm, and the length of EFPA C on the outer circumferential side is about 710 mm. The outer diameter of the ICH-EFPA is 140 mm.

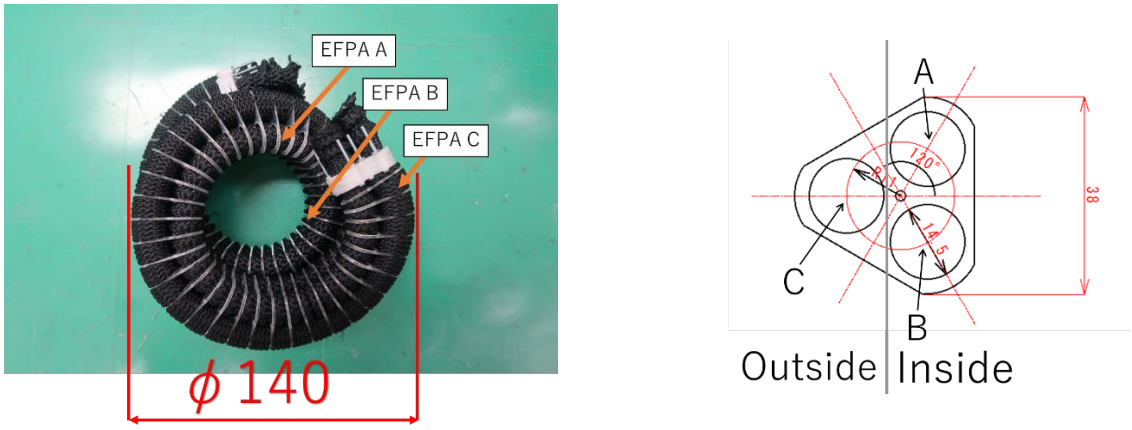

(a) view of ICH-EFPA (b) shape of restraint plate and arrangement of each EFPA

Figure 6. Construction of inner circumferential reinforced helical EFPA(ICH-EFPA).

Figure 7 shows the operation of ICH-EFPA for various pressurized pattern by using two on/off valves. The supply pressure is 500 kPa. Figure 7(a) shows the initial shape of ICH-EFPA when all EFPAs were not pressurized. Figure 7(b) shows the case when three EFPAs were pressurized. Usually, when a supply pressure of 500 kPa was applied to each EFPA, each EFPA is extended. The ICH-EFPA when all EFPAs were pressurized was almost the same as the initial ICH-EFPA as shown in Figure 7(a) and 7(b). Figure 7(c) shows the case when the outer circumferential side EFPA C was pressurized. The outer diameter of ICH-EFPA became small from 140 to 70 mm by extending EFPA C. It means that the ICH-EFPA can grasp the object in this mode. Figure 7(d) shows the case when the inner circumferential side EFPA A and B were pressurized. The ICH-EFPA became a straight shape by extending the inner circumferential side EFPAs. It means that the ICH-EFPA can release the object. As a result, the ICH-EFPA can realize both motions of grasping and releasing the object by using two on/off valves.

(a) initial state (b) pressurized to all EFPAs (c) pressurized to EFPA C

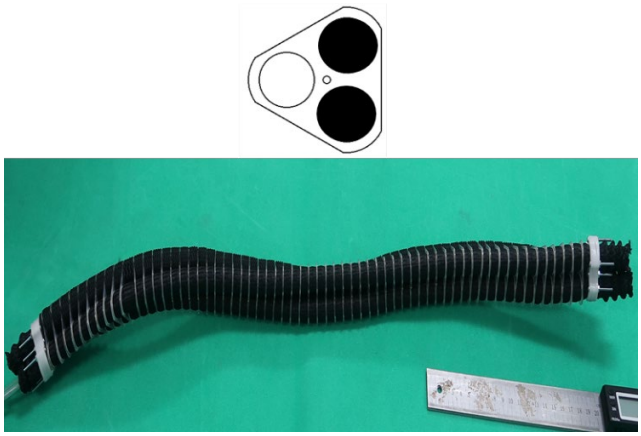

(d) pressurized to EFPAs A and B

Figure 7. Operation of ICH-EFPA for various pressurized patterns.

Outer Circumferential Reinforced Helical EFPA(OCH-EFPA)

Figure 8(a) and 8(b) show the construction of the outer circumferential reinforced helical EFPA (OCH-EFPA) and the arrangement of each EFPA of the OCH-EFPA, respectively. Compared with ICH-EFPA, the OCH-EFPA has the opposite configuration of EFPA, that is, one EFPA is arranged on the inner circumferential side and two EFPAs are arranged on the outer circumferential side. The length of EFPA A and B on the outer circumferential side is 620 mm and the length of EFPA C on the inner circumferential side is about 500 mm. The outer diameter of the ICH-EFPA is smaller, that is about 130 mm because the tightening force becomes stronger.

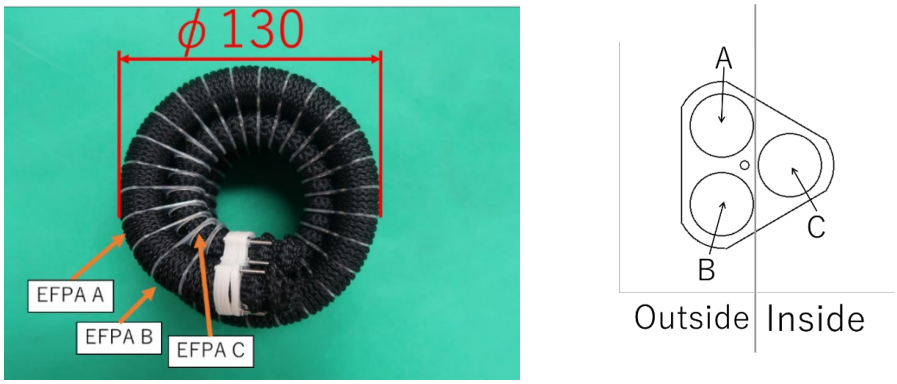

(a) view of OCS_EFPA (b) arrangement of each EFPA

Figure 8. Construction of outer circumferential reinforced helical EFPA(OCH-EFPA).

Figure 9 (a), 9(b), 9(c) and 9(d) show the operation when the initial condition with no pressurized EFPA, the case when all EFPAs were pressurized, the case when the inner circumferential side EFPA C was pressurized, and the case when the outer circumferential side EFPAs A and B were pressurized, respectively. Compared with the ICH-EFPA, in the case when all EFPAs were pressurized as shown in Figure 9(b), the outer diameter of OCH-EFPA became smaller from 130 to 65 mm. It is because the tightening force became stronger. For the same reason, when the outer circumferential side EFPAs A and B were pressurized, the outer diameter of OCH-EFPA became much smaller, as shown in Figure 9 (d). However, by being decreased extensional force of the inner circumferential side EFPA C, the OCH-EFPA can not extend to the straight shape surly, as shown in Figure 9(c).

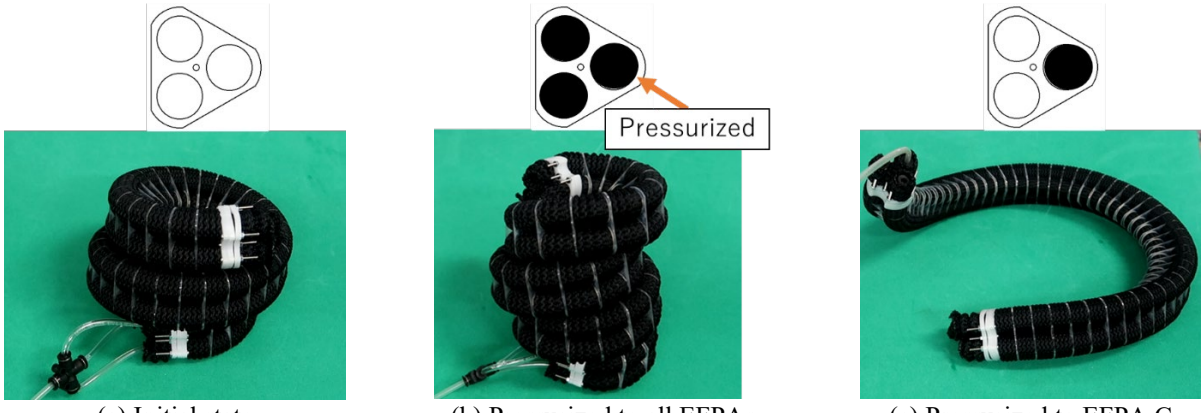

(a) Initial state (b) Pressurized to all EFPAs (c) Pressurized to EFPA C

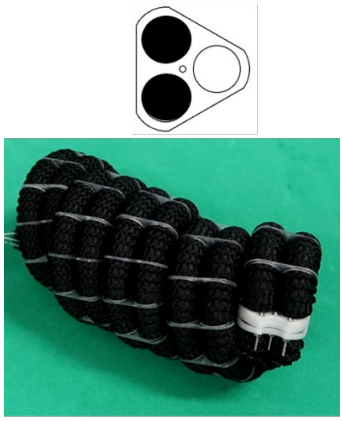

(d) Pressurized to EFPAs A and B

Figure 9. Operation of OCH-EFPA for various pressurized patterns.

Characteristics of Grasping Force of Grasping actuator using EFPAs

Figure 10 shows the view of experimental setup to measure the grasping force of the ICH-EFPA and OCH-EFPA. In the Experiment, the end of each EFPA was fixed a vise, and a plastic bottle with a diameter of 60 mm connected with the force sensor was wrapped by each EFPA. As a grasping force of the EFPA, the maximum pulling force when the plastic bottle got out of the EFPA, was measured when the outer circumferential side EFPA was pressurized from 0 to 500 kPa every 50 kPa in each EFPA. The measurement with each supply pressure was carried out 20 times. Figures 11(a) and 11(b) show the results of grasping force using the ICH-EFPA and OCH-EFPA, respectively. In both figures, the circle shows the average grasping force. Each bar shows the distribution of measured data. From both figures, it could be seen that the grasping force of both EFPA was almost the same under the condition of input pressure of less than 250 kPa. It was also found that the grasping force of the OCH-EFPA was larger than that of the ICH-EFPA in the range of higher pressure of more than 300 kPa. The maximum average grasping force of the ICH-EFPA and OCH-EFPA was about 9.2 N at 250 kPa and 11.9 N at 450kPa, respectively. In the case using the ICH-EFPA, it seemed that the deviation of grasping force of the ICH-EFPA at 450 kPa was large because it grasped the bottle irregularly. The frictional force of the ICH-EFPA is also changed in every measurement of the grasping force by this grasping. The grasping force became maximum when the supply pressure of 250 kPa was applied. This is because both EFPAs could not keep the uniform helical shape over the supply pressure of more than 300 kPa as shown in Figure 13; that is, Figure 13 shows the appearance of the ICH-EFPA when each pressure was applied. It means that both EFPAs have desirable properties for soft grasping without damage, that is, the grasping force has a limitation of around 10 N even if the supply pressure becomes higher. As a result, it is concluded that the ICH-EFPA is suitable to apply to pillar grasping flexible robot arm. The ICH-EFPA can deform a more straight shape for grasping the pillar while approaching and releasing it while away.

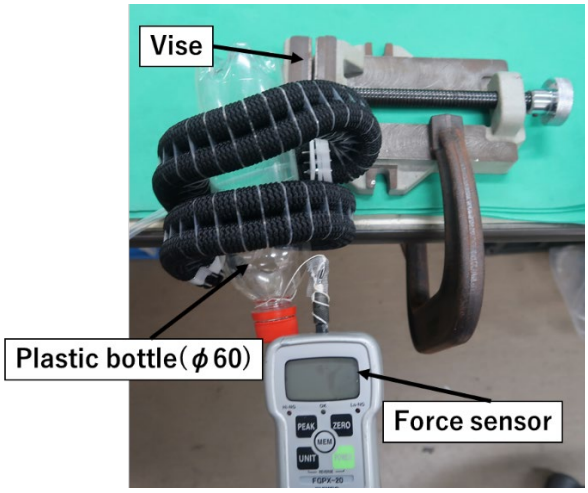

Figure 10. View of experimental setup to measure grasping force of actuators.

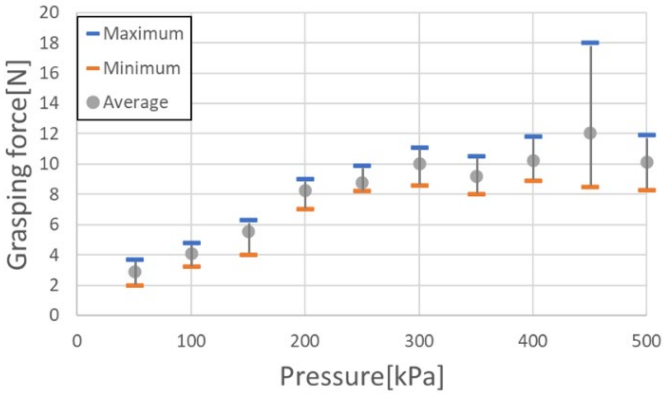

(a)

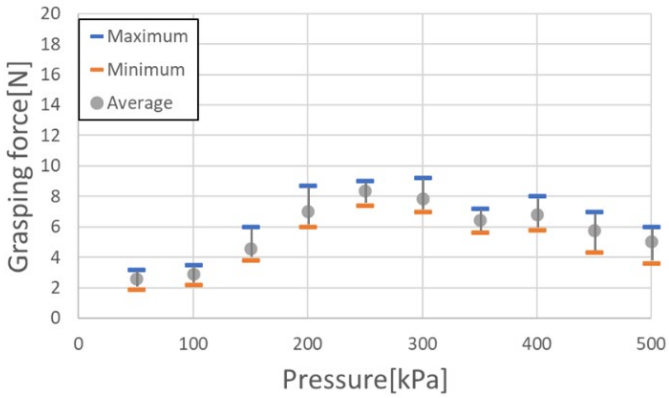

(b)

Figure 11. Results of grasping force using (a) ICH-EFPA, and (b) OCH-EFPA.

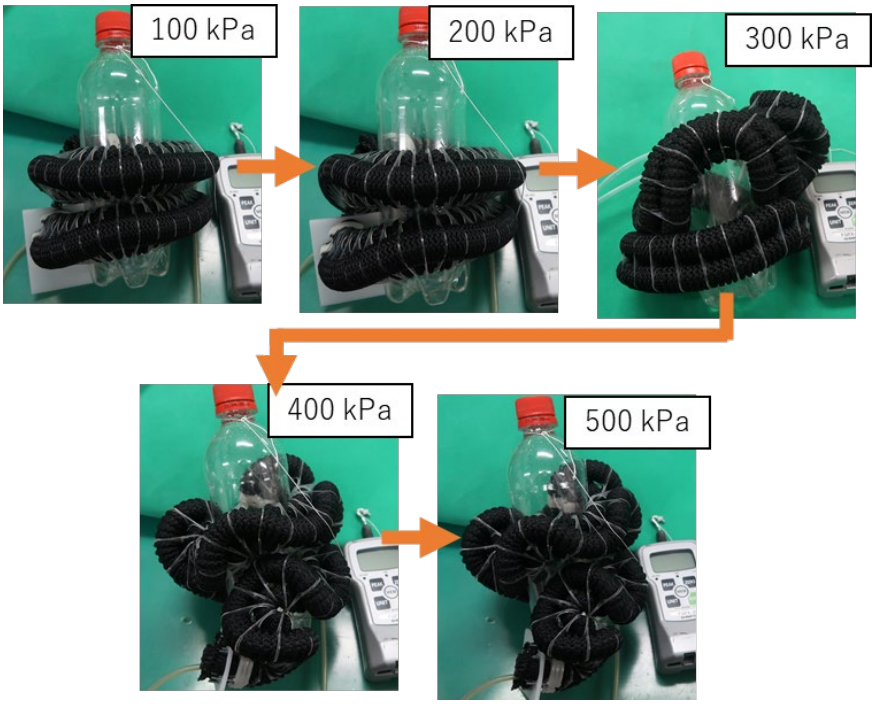

Figure 12. Appearance of the ICH-EFPA for various supply pressure.

AUTOMATIC LADDER-CLIMBING ROBOT

Pillar Grasping Flexible Robot Arm

To construct the automatic ladder climbing robot, the ladder pillar grasping flexible robot arm is required. The robot arm needs to grasp the pillar while approaching and release it while away by using two on/off operations. Based on the requirement mentioned above, the specifications of the robot arm were decided as follows.

i. The robot arm can grasp the pillar while the tip of the arm moves along logarithmic spiral trajectory.
ii. The robot arm can release the pillar while the tip of the arm moves along logarithmic spiral trajectory.
iii. The robot arm can realize both motions by using two on/off valves.
iv. The robot arm can be kept hooked on the pillar with no input as a safety.

To realize both motions of specifications i) and ii), the robot arm needs to extend toward the longitudinal direction. The robot arm also needs to bend toward the pillar for grasping and bend backward for releasing. Therefore, we consider the robot arm that combines the ICH-EFPA and the typical reinforced EFPA; that is, both EFPAs are connected in serial. In addition, to meet specification iv), the tip of the robot arm needs to have a semicircular shape to hook on the pillar without input pressure. From the viewpoint of stiffness for grasping, the semicircular-shaped ICH-EFPA is also suitable. Based on the design concept mentioned above, the pillar grasping flexible robot arm is proposed and tested. Figure 13 shows the appearance of the tested robot arm. The tested robot arm consists of the typical reinforced EFPA that is reinforced in every one-bellow and a semicircular-shaped ICH-EFPA. Figure 14(a), 14(b) and 14(c) show the operation of the tested robot arm in case of no supply pressure, case when the outer circumferential side EFPA was pressurized and case when the inner circumferential side EFPAs was pressurized, respectively. From Figure 14(b), it could be seen that the robot arm could bend backwards for releasing. From Figure 14(c), it was found that the robot arm could grasp the pillar. The robot arm could be operated by pressurizing either the inner or outer EFPA. It means that the robot arm can be controlled by using two on/off valves; that is, it means specification iii).

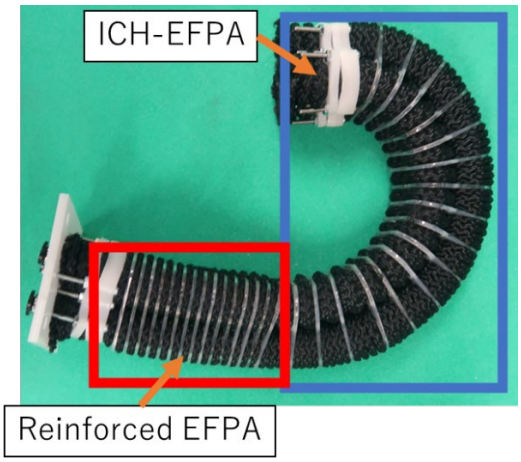

Figure 13. Appearance of the pillar grasping flexible robot arm.

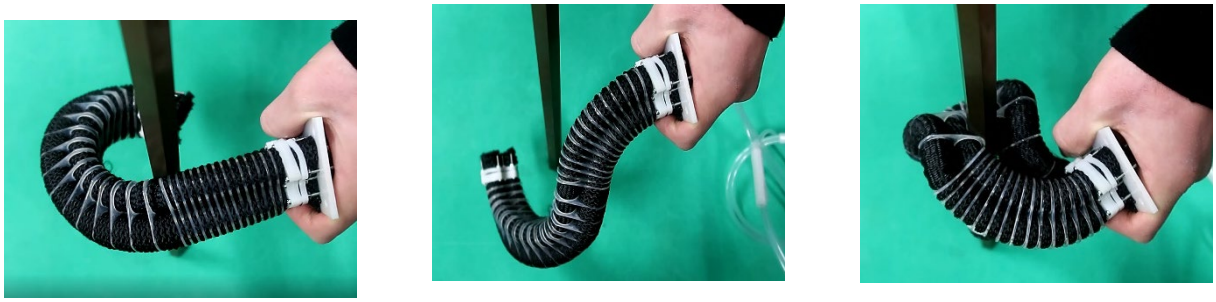

(a) No pressurized (b) Inner EFPAs pressurized (c) Outer EFPA pressurized

Figure 14. Operation of the tested robot arm using two on/off valves.

Construction and Control System of Automatic Ladder Climbing Robot

Figure 15 shows the appearance of the tested automatic ladder-climbing robot. In order to lift up and down the tested robot, the typical reinforced EFPA was used as a flexible lifting robot arm. The tested robot consists of a hexagonal column-shaped plastic frame, two pillar grasping flexible robot arms and a flexible lifting robot arm whose natural length of EFPAs is 200 mm. The lifting robot arm was set on the center side face of the hexagonal column-shaped frame. In both sides, two pillar grasping flexible robot arm were set. The pillar grasping robot arms were also installed sponges to prevent slip on pillars. The tip of the lifting arm had a rectangular-shaped hook to catch the step easily. The tested robot has a length of 480 mm, width of 440 mm and height of 55 mm. The mass of the robot is about 600 g. As the lifting robot arm required three motions, that is bending toward step for grasping step, bending backward for releasing step and extension/contraction for lifting up/down, the arm can be controlled by two on/off valves.

Figure 16 shows the schematic diagram of control system of the automatic ladder-climbing robot. The system consists of the tested robot, four on/off valves (Koganei Co. Ltd., G010E-1), an embedded controller (Renesas Co. Ltd., SH7125) and a serial communication unit (FTDI Co. Ltd., FT234X). Figure 17 shows the connection between each valve and each EFPA. The valve of No. 1 is connected to two inner circumferential side EFPAs in the lifting robot arm for bending backwards. The valve of No.2 is connected to the outer circumferential side EFPA in the lifting robot for grasping the

step. The valve of No.3 is connected to four inner circumferential side EFPAs in both pillar grasping robot arms for releasing both pillars. The valve of No.4 is connected to two outer circumferential side EFPAs in both pillar grasping robot arms for grasping both pillars. The tested robot can realize various motions by combination of activated valves. For example, the lifting robot arm can extend when both valves of No.1 and No.2 are driven. The operation of the tested robot is done as follows. First, the embedded controller gets a code through the serial communication unit from PC. The controller selects a sequential program according to the received code. Each on/off valve is driven based on the selected sequence program. Therefore, the tested robot can be realized that climbs up and down a ladder driven by using only four valves.

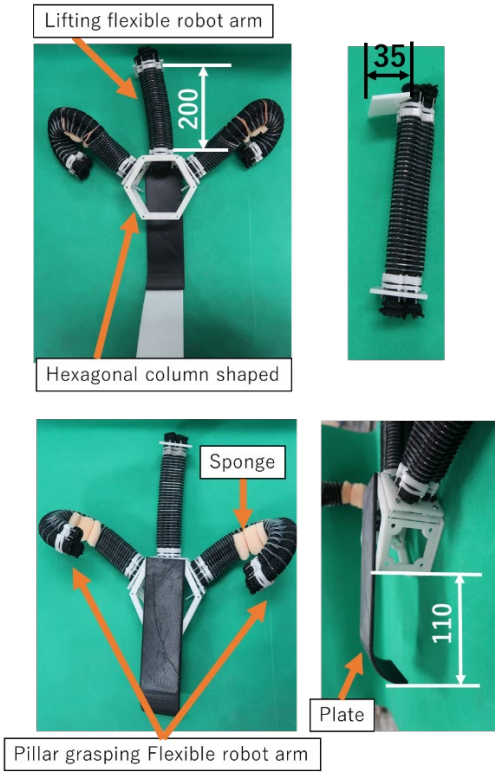

Figure 15. Appearance of the tested automatic ladder climbing robot.

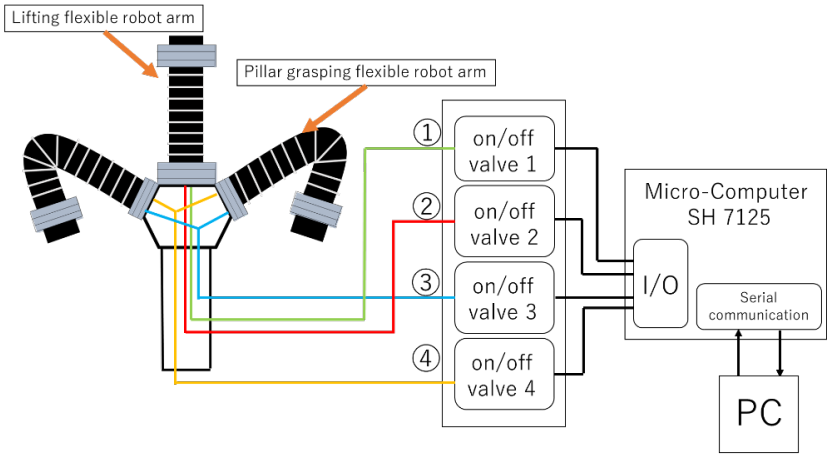

Figure 16. Schematic diagram of automatic ladder climbing system.

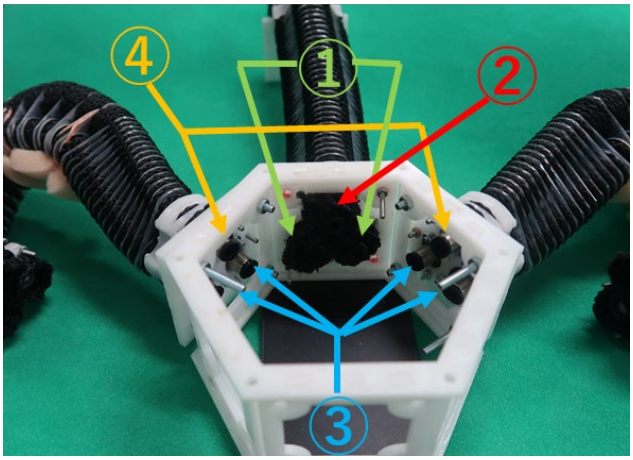

Figure 17. Connection between each valve and each EFPA.

Ladder-Climbing Up and Down Experiment using the Tested Robot

Figure 18 shows the time chart of activated valves for climbing ladder. Figure 19 shows the transient view when the tested robot climbs up the ladder. In both figures, each number enclosed in a square, that is 1 to 6, shows the attitude in each process of ladder-climbing up. The process of climbing up the ladder using the robot is as follows. At the beginning of climbing the ladder, the lifting robot arm and two pillar grasping robot arms in the robot hold two pillars and the step, as shown in Figure 19(1). Next, the lifting robot arm bends backwards while the pillar grasping robot arms are grasping two pillars as shown in Figure 19(2). In order to catch the upper step, the lifting robot arm extends by pressurizing all EFPAs in the arm, as shown in Figure 19(3). After that, as shown in Figure 19(4), the lifting robot arm grasps the upper step by bending toward the ladder. After grasping the upper step, two pillar grasping robot arms become original shape by all EFPAs are exhausted. While the lifting robot arm is also pulling up by its bending motion, two pillar grasping robot arms are bent backward as shown in Figure 19(5), in order to release pillars and avoid pillar supports.

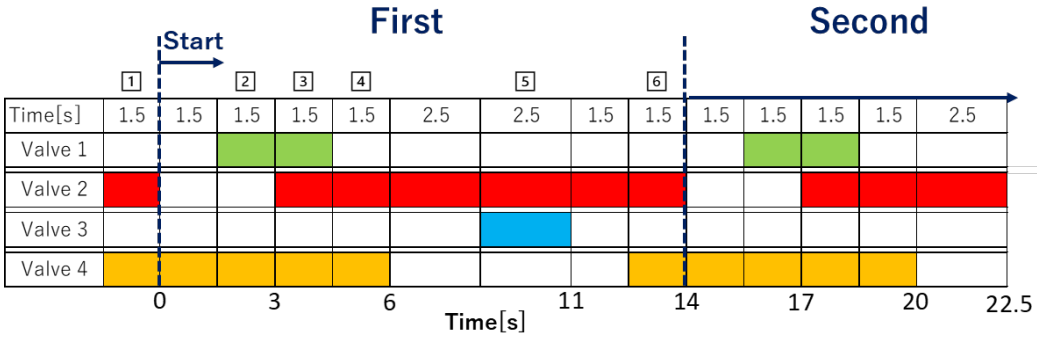

Figure 18. Time chart of activated valves for climbing ladder up.

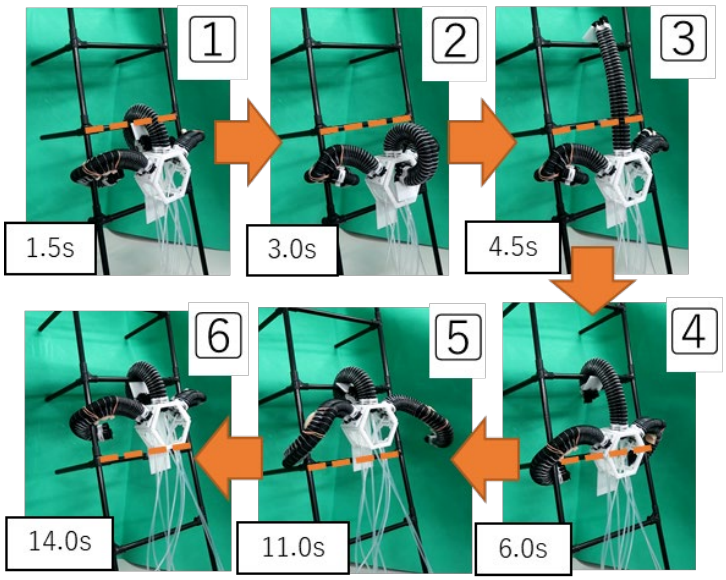

Figure 19. Transient view when the tested robot climbs the ladder up.

After the robot is climbing up by the lifting robot arm, both pillar grasping robot arms hold pillars again, as shown in Figure 19(6). By repeating these motions, the tested robot can climb the ladder. The second procedure is carried out for climbing up the ladder according to pillars where there is no pillar support. As a result, it could be found that the tested robot could climb the ladder while the robot was avoiding pillar support. The robot could climb the ladder in 14 seconds per one step climbing by using only four on/off valves. In addition, it had not been observed that the robot fell from the ladder even if the lifting robot arm missed to catch the upper step. By retrial procedure based on the time chart, the robot could climb the ladder surely. It was also found that the robot could grasp the pillar softly so as not to cause damage.

In addition, Figure 20 shows the time chart of activated valves for climbing the ladder down. Figure 21 shows the experimental result of going down of the tested robot. In both figures, each number enclosed in square, that is 1 to 6, shows the attitude in each process of ladder-climbing down. The procedure of climbing down the ladder using the robot is similar to the reverse motion of climbing up, that is as follows. In the beginning, the lifting robot arm grasps the step before climbing down. Under the condition, when the lifting robot arm keeps holding the step, both pillar grasping robot arms are bent backwards to avoid pillar support and any other obstacles, as shown in Figure 21(1). Next, both pillar grasping robot arms keep their original shapes without input pressure. In the condition, the tips of both pillar grasping robot arms naturally hook both pillars, as shown in Figure 21(2). After that, the lifting robot arm extends so as to climb down as shown in Figure 21(3). Next, both pillar grasping robot arms start to grasp both pillars. In the condition, both pillar grasping robot arms can slide according to both pillars up to the lower step. Under the condition, when both pillar grasping robot arms grasp pillars, the lifting robot arm grasps the lower step as shown in Figure 21(4). In order to grasp the step surely, the lifting robot arm changes its original shape temporally and grasps the step again. In the second procedure, to avoid pillar support and obstacles, both pillar grasping robot arms bend backwards. And the robot continues to carry out the procedure for climbing down. As a result, it could be found that the tested robot could climb the ladder down. It could be concluded that the tested ladder-climbing robot could climb the ladder up and down while avoiding the pillar supports and obstacles that require complex motion by using only four on/off valves.

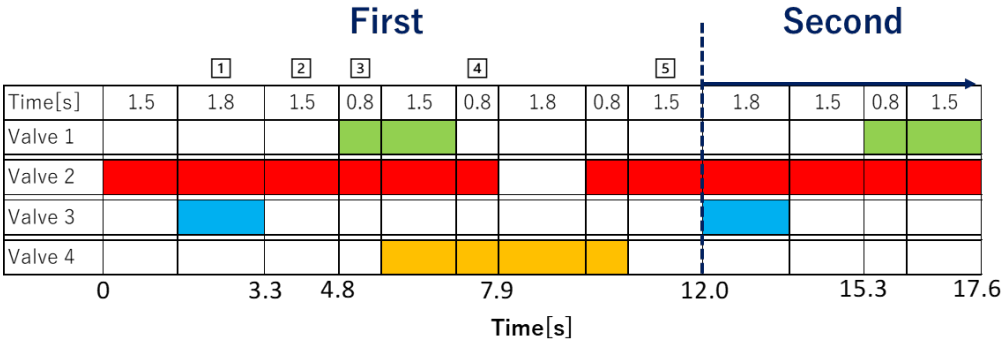

Figure 20. Time chart of activated valves for climbing the ladder down.

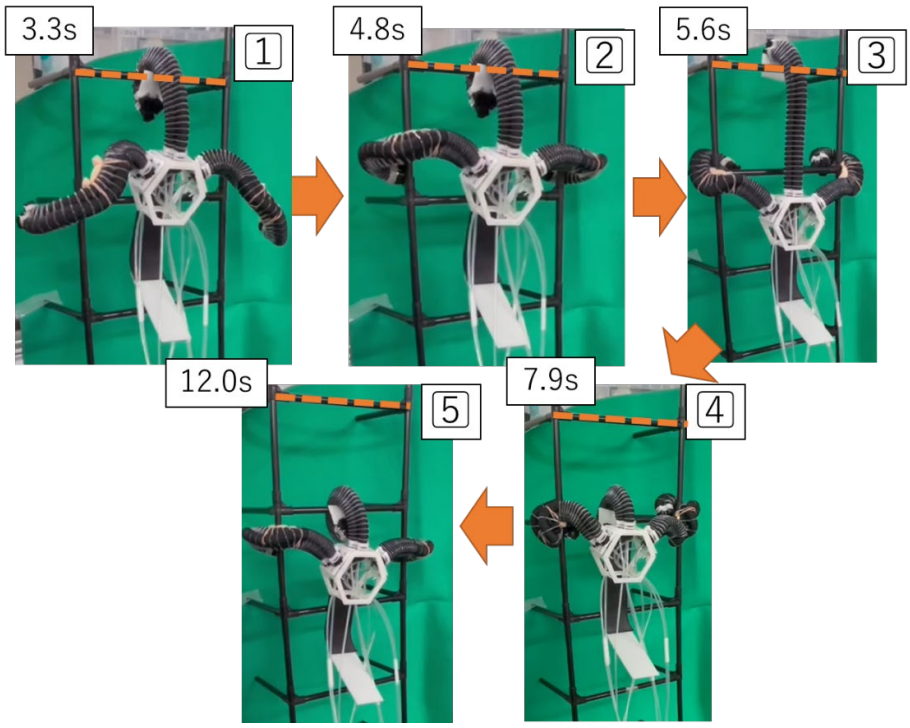

Figure 21. Transient view when the tested robot climbs the ladder down.

CONCLUSION

This study aims to develop a sequential controlled automatic ladder-climbing robot that can climb a deteriorated ladder under the condition of bad weather and be operated by only few simple valves is summarized as follows:

In order to realize both grasping and releasing the object by using only one actuator, both inner and outer circumferential reinforced helical EFPAs, that is ICH-EFPA and OCH-EFPA, were proposed and tested. As a result, it could be confirmed that both EFPAs could grasp an object by pressurizing the outer side EFPA and release an object by pressurizing the inner side EFPA.

The grasping force of ICH-EFPA and OCH-EFPA were investigated. As a result, it could be concluded that both EFPAs could grasp the object without damage because the grasping force had a limitation of around 10 N even if the supply pressure became higher. It was also found that the ICH-EFPA was suitable to apply to the pillar grasping flexible robot arm because it could deform a more straight shape for releasing the pillar.

The flexible robot arm that can grasp and release ladder pillars by using two on/off valves was proposed and tested. The automatic ladder-climbing robot with sequential control that consists of two pillar grasping robot arms and the reinforced EFPA as a lifting robot arm was also proposed and tested. In the ladder-climbing experiment, the time chart of activated valves for the robot climbing up and down was investigated by trial and error. As a result, it was confirmed that the tested robot could climb up and down the ladder by using four on/off valves without giving damage to the object.

As a future work, we are going to construct the analytical model of the flexible robot arm that can grasp and release the object for the optimal design. In addition, we are also going to consider an application using the proposed robot arm.

ACKNOWLEDGEMENT

This work was supported by JSPS KAKENHI Grant Numbers 16K06202 and 19K04265.

REFERENCES

[1] Summary of the White Paper on Land, Infrastructure, Transport and Tourism in Japan, 2020 [Online] Available: https://www.mlit.go.jp/hakusyo/mlit/r01/hakusho/r02/pdf/English%20Summary.pdf ; [Accessed: Feb 12, 2021].

[2] T. Yamaguchi, "Life cycle management of bridge structures," In: The Proceedings of the Symposium on Evaluation and Diagnosis, Japan, pp. 6-9; 2010.

[3] Ministry of Land, Infrastructure, Transport and Tourism, Bridge periodic inspection procedure [Online]. Available: https://www.mlit.go.jp/road/sisaku/yobohozen/tenken/yobo3_1_6.pdf; [Accessed: Feb. 12, 2021].

[4] Kyosei Industry Co. Ltd., Chimney inspection investigation example [Online]. Available: https://www.entotsu.biz/check/; [Accessed: Feb. 22, 2021].

[5] Y. Takada, K. Kirimoto, T. Tajiri, and T. Kawai, "Development of a bridge inspection robot working in three-dimensional environment," *Trans. Jpn. Soc. Mech. Eng. C*, 2013, vol. 79, no. 805, p. 3135-3146, doi: 10.1299/kikaic.79.3135.

[6] Y. Takada, S. Ito, and N. Imajo, "Development of a bridge inspection robot capable of traveling on splicing parts," *Inventions*, 2017, vol. 2, no. 22, p. 1-13, doi: 10.3390/inventions2030022.

[7] Y. Matsumura *et al.*, "Development of magnetic bridge inspection robot aimed at carrying heavy loads," *Int. J. Robotic Eng.*, 2018, vol. 3, no. 2, p. 1-10, doi: 10.35840/2631-5106/4110.

[8] T. Yoshiike *et al.*, "Development of experimental legged robot for inspection and disaster response in plants," In IEEE/RSJ *IEEE Int. Conf. Intell. Robots Syst.* (IROS), Canada, 2017, p. 4869-4876, doi: 10.1109/IROS.2017.8206364.

[9] T. Yoshiike *et al.*, "The experimental humanoid robot E2-DR: A design for inspection and disaster response in industrial environments," *IEEE Robot Autom. Ma.g*, 2019, vol. 26, no. 4, p. 46-58, doi: 10.1109/MRA.2019.2941241.

[10] K. Hashimoto *et al.,* "A four-limbed disaster-response robot having high mobility capabilities in extreme environments," In: *IEEE Int. Conf. Intell. Robots Syst* (IROS 2017), Canada, 2017, p. 5398-5405, doi: 10.1109/IROS.2017.8206436.

[11] K. Asa, Y. Funabora, S. Doki, and K. Doki, "Automatic measuring position determination of uavs for visual inspection system of infrastructures based on 3D construction model considering accuracy of data," *Trans. Soc. Instrum. Control Eng.*, 2017, vol. 53, no. 3, p. 229-235, doi: 10.9746/sicetr.53.229.

[12] K. Asa, Y. Funabora, S. Doki, and K. Doki, "Measuring position determination of uav for visual inspection system ensuring accuracy and considering efficiency of data-gathering," *Trans. Soc. Instrum. Control Eng.*, 2019, vol. 55, no. 5, p. 386-392, doi: 10.9746/sicetr.55.386.

[13] A. Saputra, Y. Toda, N. Takesue and N. Kubota, "A novel capability of quadruped robot moving through vertical ladder without handrail support," In: *IEEE Int. Conf. Intell. Robots Syst.,* (IROS), China, 2019, p. 1448-1453, doi: 10.1109/IROS40897.2019.8968175.

[14] Y. Suzuki *et al.*, "Development of tetrahedral type rehabilitation device using flexible pneumatic actuators," *Int. J. Mech. Eng. Robot. Res.*, 2018, vol. 7, no. 4, p. 409-414, doi: 10.18178/ijmerr.7.4.409-414.

[15] K. Kusunose *et al.*, "Development of pipe holding mechanism and bending unit using extension type flexible actuator for flexible pipe inspection robot," *Int. J. Mech. Eng. Robot. Res*., 2019, vol. 8, no. 1, p. 129-134, doi: 10.18178/ijmerr.8.1.129-134.

[16] S. Shimooka *et al.*, "Improvement of home portable rehabilitation device for upper-limbs," *JFPS International Journal of Fluid Power System*, 2019, vol. 12, no. 1, p. 10-18, doi: 10.5739/jfpsij.12.10.

[17] K. Kusunose *et al.*, "Development of inchworm type pipe inspection robot using extension type flexible pneumatic actuators," *Int. J. Automot. Mech.*, 2020, vol. 17, no. 2, p. 8019-8028, doi: 10.15282/ijame.17.2.2020.20.0601.

[18] S. Shimooka *et al.*, "Development and attitude control of washable portable rehabilitation, device for wrist without position sensor," *JFPS International Journal of Fluid Power System*, 2020, vol. 13, no. 3, p. 25-34, doi: 10.5739/jfpsij.13.25.

[19] S. Shimooka *et al.*, "Development of reinforced extension type flexible pneumatic actuator with circumferential restraints and its application for rehabilitation device," *Int. J. Automot. Mech.*, 2020, vol. 17, no. 3, p. 8116-8127, doi: 10.15282/ijame.17.3.2020.05.0609.